Journal of Solid State Chemistry **163,** 286–293 (2002)
doi:10.1006/jssc.2001.9410, available online at http://www.idealibrary.com on IDEAL®

Defects and Luminescence Behavior of Cubic *F23* $[(NH_4(18\text{-Crown-6}))_4MnX_4]\ [TlX_4]_2$ (X = Cl, Br) Crystals

Nicolette S. Fender[1] and Ishenkumba A. Kahwa[2]

Department of Chemistry, University of the West Indies Mona Campus, Kingston 7, Jamaica, West Indies

and

Frank R. Fronczek

Department of Chemistry, Louisiana State University Baton Rouge, Louisiana 70803

Received May 16, 2001; in revised form September 20, 2001; accepted 27, 2001

Luminescence from $[(NH_4(18\text{-Crown-6}))_4MnBr_4][TlBr_4]_2$ (1), $[(NH_4(18\text{-Crown-6}))_4MnCl_4][TlCl_4]_2$ (2), $[(NH_4(18\text{-Crown-6}))_2MnBr_4]$ (3), and $[(NH_4(18\text{-Crown-6}))_2MnCl_4]$ (4) was studied in search of new insights regarding crystal defects in 2. Emission from 3 and 4 is normal $Mn^{2+}(^4T_1(^4G) \rightarrow {}^6A_1)$; that of 2 ($\lambda_{max} \approx 520$ nm at ca. 300 K and 560 nm at 77 K) is unusual and temperature dependent. Thermal barriers (kJ/mol, assignment): green emission of 1 and 2, $T < 150$ K (1–2, NH_4^+ rotations), $150 < T < 250$ K (7–14, energy migration among $[MnX_4]^{2-}$), $250 < T < 300$ K (26–35, rotations of 18-Crown-6)); yellow emission of 2: $T < 250$ K (7–8, energy migration among $[MnX_4]^{2-}$), $T > 250$ K (29 kJ/mol, defect-to-$Mn^{2+}(^4T_1(^4G))$ back energy transfer). Crystal data for 4: Space group $P2_1/c$; $Z = 4$; $a = 20.173(1)$ Å; $b = 9.0144(8)$ Å; $c = 20.821(1)$ Å; $\beta = 98.782(5)^\circ$; $V = 3741.9(8)$ Å^3; $R_w = 0.059$; $R = 0.054$. © 2002 Elsevier Science

Key Words: **supramolecular aggregations; manganese(II) luminescence; tetrahalomanganate(II); energy transfer; 18-Crown-6; crystal defects.**

INTRODUCTION

Cubic $F23$ manganese(II) supramolecular assemblies of core stoichiometry $[(A(18\text{-Crown-6}))_4MnX_4][BX_4]_2$ (X = Cl, Br; $A^+ = K^+, Rb^+, Tl^+, [NH_4]^+$ or other mono-cation; B = Tl, Fe) have a propensity for occlusion of photonically active crystal defects (1–4(a), 5). Structural details of these cubic supramolecular materials were discussed previously (1–3, 5, 6); for clarity of this presentation essential interactions in the key $[(A(18\text{-Crown-6}))_4MnX_4]^{2+}$ cations are shown for one of the four (K(18-Crown-6))-to-$MnBr_4$ supramolecular links in $[(K(18\text{-Crown-6}))_4MnBr_4][TlBr_4]_2$ (3, 6) (Fig. 1). Preliminary studies on corresponding ammonium salts (3) revealed that while bromide $[(NH_4(18\text{-Crown-6}))_4MnBr_4][TlBr_4]_2$ (**1**) features $Mn^{2+}(^4T_1(^4G) \rightarrow {}^6A_1)$ green emission typical of ca. T_d $[MnBr_4]^{2-}$ anions ($\lambda_{max} \approx 512$ nm), which is somewhat quenched, the chloride $[(NH_4(18\text{-Crown-6}))_4MnCl_4][TlCl_4]_2$ (**2**) exhibits an intriguing temperature dependent emission with $\lambda_{max} \approx 520$ nm at 298 K and 560 nm at 77 K. It was thus interesting to study the luminescence decay dynamics of **1** and **2** in detail in search of new insights into factors governing those intriguing emission characteristics. Emission characteristics of $[(Rb(18\text{-Crown-6}))_4MnBr_4][TlBr_4]_2$ (3), $[(Rb(18\text{-Crown-6}))_4MnCl_4][TlCl_4]_2$ (4a) and $[(Tl(18\text{-Crown-6}))_4MnCl_4][TlCl_4]_2$ (4a), which exhibit only the normal $Mn^{2+}(^4T_1(^4G) \rightarrow {}^6A_1)$ emission of ca. T_d $[MnBr_4]^{2-}$ anions, as well as those of $[(K(18\text{-Crown-6}))_4MnBr_4][TlBr_4]_2$ (which features only the strange yellow emission) (3) have been studied previously and found to be associated with defect activity. Therefore, the behavior of compound **2** is most provocative because it is thus far the only such cubic $F23$ member to simultaneously exhibit both the normal green Mn^{2+} $(^4T_1(^4G) \rightarrow {}^6A_1)$ emission of ca. T_d $[MnBr_4]^{2-}$ anions and the strange yellow one of crystal defect origin. Understanding the decay dynamics of the luminescence behavior of compound **2**, especially the relationship between the normal and strange emissions, is therefore crucial because there lies the potential for new and more informative data about the defects in cubic $F23$ systems. Further, it is possible for the detailed nature of the crystal electric field at the Mn^{2+} sites (hence electronic behavior) in compounds **1** and **2** to be influenced by defects such as $[(A(18\text{-Crown-6}))_n MnX_4]^{(n-2)+}$ ($n < 4$) associated with differences in numbers and modes of $[NH_4(18\text{-Crown-6})]^+$ - to - $[MnX_4]^{2-}$

[1] Current address: IBM–Almaden Research Center, 650 Harry Road, San Jose, CA, 95120.

[2] To whom correspondence should be addressed. Fax: (876) 977 1835. E-mail: ikahwa@uwimona.edu.jm.

0022-4596/02 $35.00

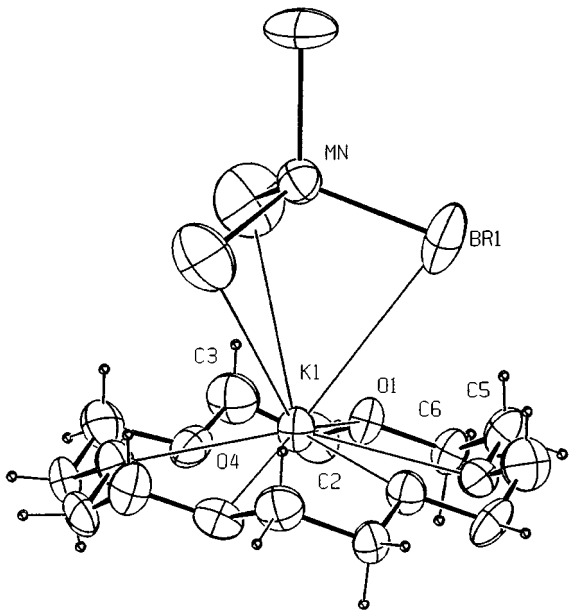

FIG. 1. One of the four $[K(18\text{-Crown-6})]^+$ cations bound to triangular faces of T_d $[MnBr_4]^{2-}$ ions in cubic $F23$ $[(K(18\text{-Crown-6}))_4MnBr_4][TlBr_4]_{2(s)}$.

supramolecular links. Such defects can exert electronic behavior of their own or generate charge imbalances that may require placement of Mn^{2+} ions in strange environments of the cubic $F23$ crystal system in which they could be luminescent or just good energy acceptors/donors. For this reason, the synthesis of $[(NH_4(18\text{-Crown-6}))_3MnX_4][TlX_4]$ and $[(NH_4(18\text{-Crown-6}))_2MnX_4]$, which have fewer such links and are possible intermediates in a stepwise assembly of cubic $F23$ $[(NH_4(18\text{-Crown-6}))_4MnX_4][TlX_4]_2$, were sought so that their electronic behaviors can be compared with those of **1** and **2**. Herein we report the luminescence spectral and decay dynamical behavior of **1**, **2**, $[(NH_4(18\text{-Crown-6}))_2MnBr_4]$ (**3**) and $[(NH_4(18\text{-Crown-6}))_2MnCl_4]$ (**4**), as well as the molecular structure of **4**.

EXPERIMENTAL

Materials

Potassium bromide was of purity $> 99.5\%$ from BDH Chemicals Ltd., rubidium bromide and rubidium chloride salts were prepared by neutralizing 99.99% rubidium carbonate (from Aldrich) with concentrated hydrobromic and hydrochloric acid, respectively, and then evaporating off the excess acid to give the crystalline halide. Ammonium bromide was 99% pure from BDH while ammonium chloride was 99.5% pure from Philip Harris Ltd. The manganese(II) halides as $(MnX_2 \cdot nH_2O)$ were $> 98\%$ pure from BDH while 18-crown-6, HM18-Crown-6 and DB18-Crown-6 (Chart 1) were $> 98\%$ pure from Aldrich.

Syntheses

Cubic $F23$ $[(A(18\text{-Crown-6}))_4MnX_4][TlX_4]_2$ complexes were prepared as described previously (1–4a, 5). The $[(A(18\text{-Crown-6}))_2MnX_4]$ complexes were prepared by reacting the alkali metal or ammonium halide (1 mmol) and the respective crown ether (1 mmol) in 15 cm^3 ethanol (or acetonitrile in the case of DB18-crown-6) in a 50 cm^3 conical flask. Upon heating a clear solution was obtained and 0.5 mmol of solid hydrated manganese halide was added. To the resulting clear solution *n*-butanol (10 cm^3) was added and the reaction flask then clamped to rest partially on a hot plate in order to set up a temperature gradient across the base of the flask. Crystallization of the compounds occurred on the cooler side over 2 to 3 days, following slow evaporation of ethanol at a temperature of ca. 60°C. The crystals were harvested in high yields, up to 88% for $[(K(DB18\text{-Crown-6}))_2MnBr_4]\cdot 2H_2O_{(s)}$, from the warm ethanol/butanol or acetonitrile/butanol solutions and quickly dried on tissue paper. Analyses for $[(K(DB18\text{-Crown-6}))_2MnBr_4]\cdot 2H_2O_{(s)}$, Calc.(%): C, 39.7; H, 4.3; Found (%): C, 39.54; H, 3.99. For compound $[(NH_4(18\text{-Crown-6}))_2MnCl_4]_{(s)}$, yield = 62%; analyses: Calc.(%): C, 37.9; H, 7.4; N, 3.7; Found (%): C, 37.79; H, 7.34; N, 3.60. $[(NH_4(18\text{-Crown-6}))_2MnBr_4]\cdot 2CH_3CH_2OH_{(s)}$, yield = 43%; analyses: Calc. (%): C, 32.6; H, 6.7; N, 2.7; Found (%): C, 32.49; H, 6.40; N, 2.74. $[(K(18\text{-Crown-6}))_2MnBr_4]_{(s)}\cdot 2CH_3CH_2OH$, yield = 78%; analyses: Calc.(%): Br, 29.8; C, 31.3; H, 5.6; Found (%): Br, 30.37; C, 31.13; H, 5.43. $[(Rb(18\text{-Crown-6}))_2MnBr_4]_{(s)}\cdot 2CH_3CH_2OH$, yield = 67%; analyses: Calc.(%): Br, 27.4; C, 28.8; H, 5.2; Found (%): Br, 27.57; C, 29.17; H, 5.06.

Elemental Analysis

Elemental analyses of carbon, hydrogen, bromine, and chlorine were performed by MEDAC Limited (Uxbridge, UK).

Mass Spectrometry

FAB MS was performed at Imperial College of Science, Technology and Medicine (London) using an AutospecQ spectrometer and *meta*-nitrobenzyl alcohol as the matrix. Isotopic abundance patterns were calculated using the *Sheffield ChemPuter Isotope Patterns Calculator* from Sheffield University (UK) which is accessible on the Internet at: http://www.shef.ac.uk/chemistry/chemputer/isotopes.html

Luminescence

The Perkin–Elmer Model LS-5 luminescence spectrophotometer (used to obtain emission and excitation spectra) and the Photon Technology International (PTI) PL 2300 nitrogen and a matching PL 201 dye lasers used to obtain

TABLE 1
Crystallographic Data for Compound $[(NH_4(18\text{-Crown-}6))_2MnCl_4]_{(s)}$ (4)

Empirical formula	$C_{24}H_{56}N_2O_{12}MnCl_4$
Fw	761.5
Temperature, K	298
Crystal system	monoclinic
Space group	$P2_1/c$
a, Å	20.173(1)
b, Å	9.0144(8)
c, Å	20.821(1)
β, °	98.782(5)
V, Å^3	3741.9(8)
Z, d_{calc} g/cm^3	4, 1.352
$F(0, 0, 0)$	1612
Abs. coeff. (μ), cm^{-1}	6.78
θ-limits, deg.	1–30
No. of unique reflections	10877
No. of observed reflections	7299
No. of variables	421
R (obs. data)	0.054
R_w	0.059
GOF	1.603
Max. resid. dens., eÅ^{-3}	0.57
Min. resid. dens., eÅ^{-3}	−0.15

decay curves were described previously (4a). In all cases, excitation of the MnX_4^{2-} chromophore was at $\lambda_{exc} =$ 479 nm using coumarin 481 laser dye from PTI Inc. Variable temperature measurements were accomplished using a APD Cryogenics Inc. CSW-202 Displex Helium refrigerator with the sample in contact with cryocon conducting grease.

Crystal Structure Determination

The experimental setup used to obtain structural information was described previously (3); essential crystal data and structure refinement parameters are given in Table 1 while all the structural details have been submitted to the Cambridge Crystal Data Centre.

RESULTS AND DISCUSSION

Preparation of Compounds 1–4 and the Structure of 4

The preparation of cubic $F23$ $[(NH_4(18\text{-Crown-}6))_4MnX_4][TlX_4]_2$ complexes **1** and **2** was described previously (1–4a, 5) while the new crystalline compounds of general formula $[(A(18\text{-Crown-}6^*))_2MnX_4]$ (18-Crown-6* = 18-Crown-6, HM18-Crown-6 or DB18-Crown-6, (Scheme 1), A = K, Rb, Tl, NH_4) were easily prepared in relatively high yields (see Experimental section). The new compounds were however, obtained as extensively twinned crystals, except for $[(NH_4(18\text{-Crown-}6))_2MnCl_4]$ (**4**) the crystals of which were of single crystal X-ray diffraction

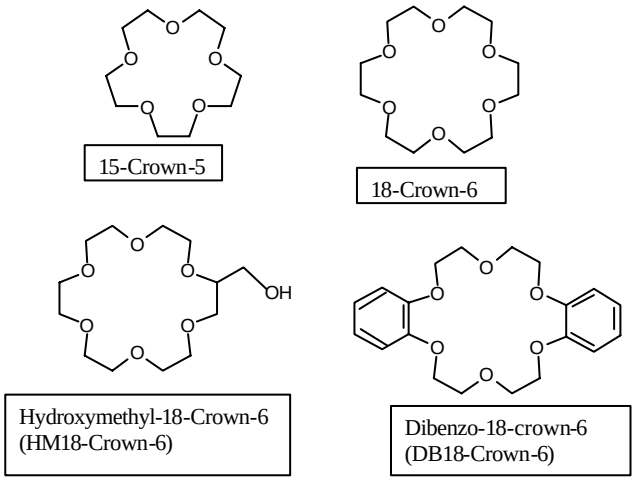

CHART 1. Relevant crown ether chelates.

quality. The structure of **4** was successfully determined thereby confirming the identity of the new $[(A(18\text{-Crown-}6^*))_2MnX_4]$ series. The molecular structure of **4** is shown in Fig. 2. Each $[(NH_4(18\text{-Crown-}6))_2MnCl_4]$ molecule features two $[NH_4(18\text{-Crown-}6)]^+$ cations of C_{3v} symmetry each of which is bound to an individual Cl atom of the $[MnX_4]^{2-}$ anion via single N–H … Cl hydrogen bonds (hereafter "vortex binding") (Fig. 2). Two of the four Cl atoms of $[MnCl_4]^{2-}$ are not engaged in N–H … Cl hydrogen bonding. This vortex binding brings to three, the number of supramolecular interaction modes by which the C_{3v} $[A(18\text{-Crown-}6)]^+$ cations can bind to T_d $[MX_4]^{2-}$ anions. In cubic $F23$ $[(A(18\text{-Crown-}6))_4MnX_4][TlX_4]_2$ (1–4a, 5) each A atom binds to the triangular face of the T_d $[MX_4]^{2-}$ anion (hereafter "facial binding") (Fig. 1). In $[Ba(18\text{-Crown-}6)(MX_4)(H_2O)n]$ ($n = 0$ or 1) the Ba^{2+} ions of the $[Ba(18\text{-Crown-}6)]^{2+}$ complex prefer binding to the edge formed by a pair of X sites of the $[MX_4]^{2-}$ anions (hereafter "edge binding") (1, 2). It was thus interesting to

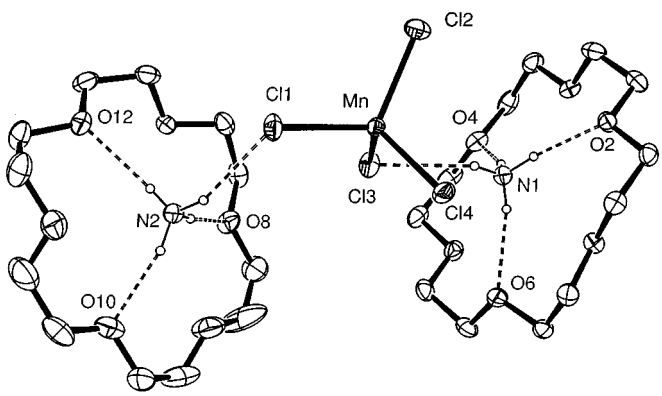

FIG. 2. Molecular structure of $[(NH_4(18\text{-Crown-}6))_2MnCl_4]_{(s)}$.

determine whether vortex (in **3** and **4**) and facial (in cubic *F*23 **1** and **2**) modes of assembling $[NH_4(18\text{-Crown-6})]^+$ cations around the $[MnX_4]^{2-}$ anions do influence differently emission, absorption, and energy transport characteristics involving Mn^{2+} sites.

Contrasting Luminescence Spectra of $[(A(18\text{-}Crown\text{-}6))_2MnX_4]_{(s)}$ *and Cubic F23* $[(A(18\text{-}Crown\text{-}6))_4MnX_4][TlX_4]_{2(s)}$

When excited by near UV or blue light crystalline complexes of general stoichiometries $[(A(18\text{-Crown-6}))_2MnX_4]_{(s)}$ and $[(A(DB18\text{-Crown-6}))_2MnBr_4]_{(s)}$, especially

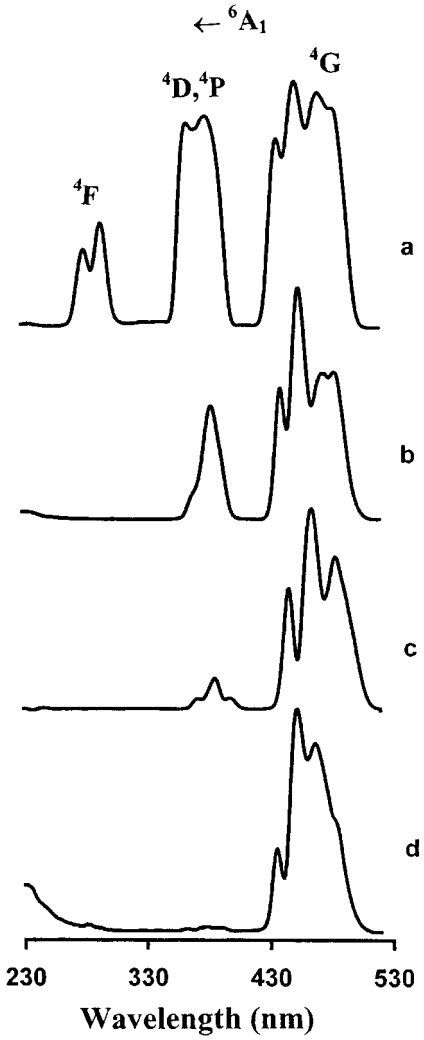

FIG. 3. A comparison of 77 K excitation spectra revealing reduced $Mn^{2+}(^4F, ^4D, ^4P \leftarrow {}^6A_1)$ transition intensities in some cubic *F*23 $[(A(18\text{-Crown-6})^*)_4MnBr_4][TlBr_4]_{2(s)}$ complexes because of inner-filter effects of strongly UV-absorbing defect sites: (a) $[(NH_4(18\text{-crown-6}))_2MnBr_4]$ (**3**) ($\lambda_{em} = 580$ nm); (b) $[(Rb(HM18\text{-Crown-6}))_4MnBr_4][TlBr_4]_2$ ($\lambda_{em} = 535$ nm); (c) $[(K(18\text{-Crown-6}))_4MnBr_4][TlBr_4]_2$ ($\lambda_{em} = 540$ or 610 nm); (d) $[(Ba(M18\text{-Crown-6}))_4MnBr_4][TlBr_4]_2$ ($\lambda_{em} = 550$ nm).

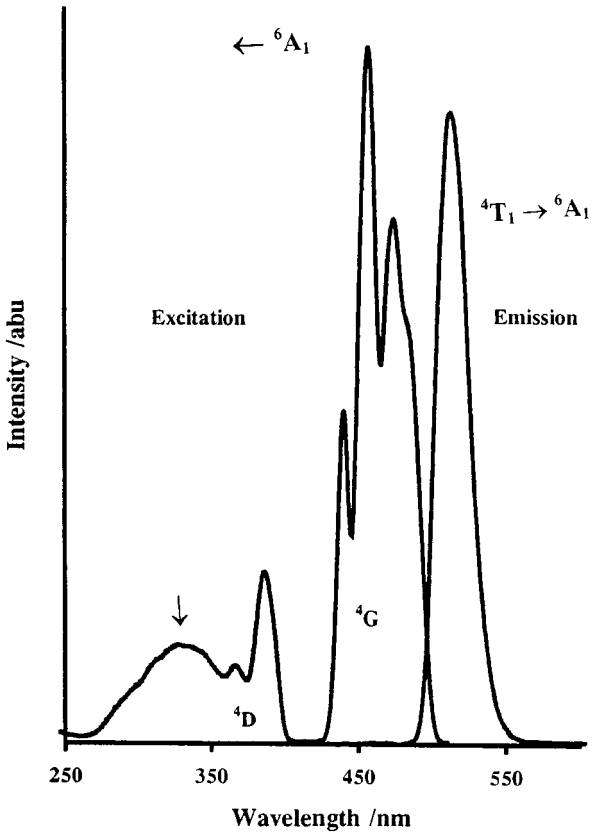

FIG. 4. 77 K excitation ($\lambda_{em} = 512$ nm) and emission ($\lambda_{ex} = 387$ nm) spectra of $[(NH_4(18\text{-Crown-6}))_4MnBr_4][TlBr_4]_{2(s)}$ (**1**) showing the unusual broad absorption (indicated by ↓ arrow) at low wavelengths and its inner-filter effect on the $Mn^{2+}(^4F, ^4D, ^4P \leftarrow {}^6A)$ transition intensities.

those corresponding to A = Rb, K, or NH_4, feature bright emission with weakly temperature dependent decay rates as normally expected for $Mn^{2+}(^4T_1(^4G) \rightarrow {}^6A_1)$ in ca. T_d $[MX_4]^{2-}$ anions. For example, the strong $Mn^{2+}(^4T_1(^4G) \rightarrow {}^6A_1)$ emission of $[(NH_4(18\text{-Crown-6}))_2MnBr_4]_{(s)}$ (**3**) peaks at ca. 512 nm and its excitation spectrum (Fig. 3a) features relatively strong transitions from the $^6A_1$ ground state to all the upper ^4G, ^4P, ^4D, and ^4F quartets. By contrast, cubic *F*23 $[(A(18\text{-Crown-6}))_4MnX_4][TlX_4]_{2(s)}$ compounds have electronically active defects the activities of which are demonstrated by the following features:

(i) A variety of spectral profiles and emission colors as shown by **1** (green) (Fig. 4), (**2**) (green at 298 K and yellow at 77 K (Fig. 5 (insert)) and other $[(A(18\text{-Crown-6}))_4MnBr_4][TlBr_4]_{2(s)}$ members (A = K (yellow), Rb (green)) (3). Compound $[(Na(18\text{-Crown-6}))_4MnBr_4][TlBr_4]_{2(s)}$ does not emit at 77 or 298 K (6).

(ii) Unusually intense UV absorptions which exert "inner-filter effects" (4) on normal Mn^{2+} transitions below 400 nm. For example, compare the normal spectral profile of $Mn^{2+}(^4F, ^4P, ^4D, ^4G \leftarrow {}^6A_1)$ absorptions of **3** (Fig. 3a) with abnormal ones from cubic *F*23 systems whose high energy

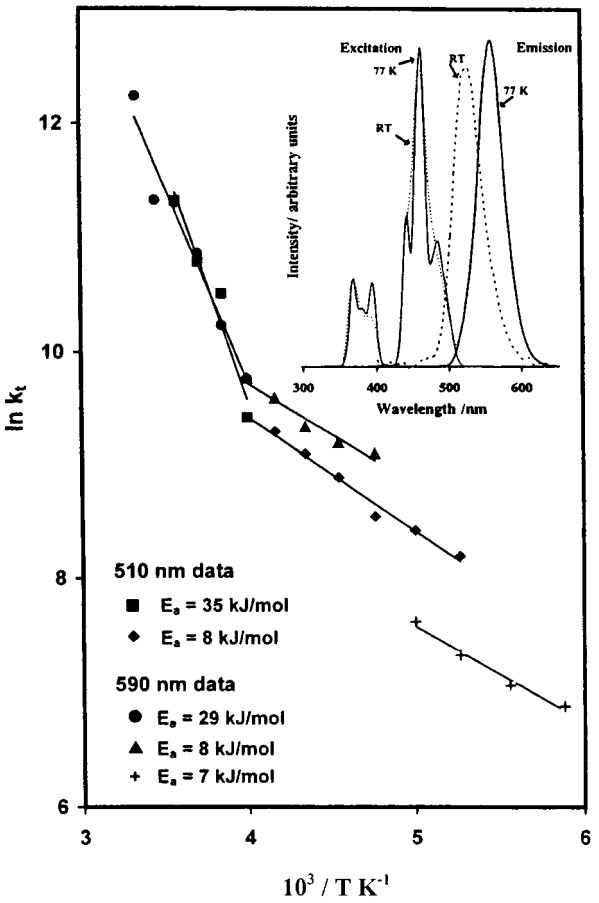

FIG. 5. Arrhenius plots (ln k_t vs $1/T$) (170–300 K) for [$(NH_4$(18-Crown-6))$_4MnCl_4$][$TlCl_4$]$_{2(s)}$ (**2**)): normal $^4T_1(^4G)$ ([$MnBr_4$]$^{2-}$) emission monitored at 510 nm while defect yellow emission was monitored at 590 nm. Inset shows the corresponding emission and excitation spectra.

absorptions are "filtered out" (Figs. 3b–3d); see also the spectra of [(Rb(18-Crown-6))$_4$MnBr$_4$][TlBr$_4$]$_{2(s)}$ in Ref. (3) (Fig. 4) and **2** in Fig. 5 (insert)).

(iii) Unusually broad absorption peaking at ca. 330 nm for compound **1** (see arrow in Fig. 4); see also the spectrum of [(Rb(18-Crown-6))$_4$MnBr$_4$][TlBr$_4$]$_{2(s)}$ (Fig. 4 in Ref. (3)).

We interpret these observations as follows: The broad UV (250–350 nm) absorption features exhibited by compounds **1** (Fig. 4) and [(Rb(18-Crown-6))$_4$MnBr$_4$][TlBr$_4$]$_{2(s)}$ (Fig. 4, Ref. (3)) are attributed to Mn^{2+} defect sites with favorable conditions for spin-orbit coupling of the ^{4}F quartet with higher energy states such as doublets of the ^2I manifold or higher energy charge transfer states. Arguments in favor of this interpretation were presented in a landmark paper by Vala *et al.* (7). Transitions between pure doublets of ^2I and the ^6A sextet states are more strictly forbidden compared to those involving the quartets and are very weak in the absence of spin-orbit coupling (7). In this case, lack of such spin–orbital coupling at relatively lower energies may explain why there are no significant inner-filter effects at wavelengths higher than 400 nm (Figs. 3b–3d) in excitation spectra of the cubic $F23$ compounds. When such broad UV-absorption from defect sites culminates in defect emission in the 500–600 nm range or energy transfer to species emitting in this region (including normal [MnX_4]$^{2-}$ anions) both the unusual broad UV-absorption and the normal Mn^{2+}(^{4}F , ^{4}D, ^{4}P) $\leftarrow {}^6A_1$) transitions may be observed (Fig. 4). Without emission from defect sites or defect –to–[$MnBr_4$]$^{2-}$ energy transfer, inner-filter effects can be expected to dominate at wavelengths lower than 400 nm and result in severely diminished or unobservable Mn^{2+}(^{4}F, ^{4}D, ^{4}P) $\leftarrow {}^6A_1$) transitions as shown in Figs. 3b–3d.

A strange yellow emission similar to that of **2** (Fig. 5 (insert)) at 77 K dominates the 77 K emission spectrum of compound [(K(18-Crown-6))$_4$MnBr$_4$][TlBr$_4$]$_{2(s)}$ which was studied in detail earlier (3) and was found to have active excitation traps and severely diminished Mn^{2+}(^{4}F, ^{4}P, ^{4}D $\leftarrow {}^6A_1$) transition intensities (Fig. 3c). We attribute the yellow 77 K emission of **2** to emissive defect sites in its cubic $F23$ crystals and the 298 K green emission to its normal Mn^{2+}($^4T_1(^4G) \rightarrow {}^6A_1$) transition of ca. T_d [MX_4]$^{2-}$ anions. Normally, when an energy donor and an acceptor of relatively lower energy are both emissive, donor emission is expected to dominate at low temperature where quenching by acceptor states should be minimal. Accordingly, lower energy acceptor emission would normally be expected to dominate at higher temperature because of efficient sensitization by energy transfer from higher energy donor states. The emission behavior of compound **2** (Fig. 5(insert)) is, from this perspective very strange, but its temperature dependence can be accounted for by reversible energy transfer between states of the green and yellow emitters. Energy transfer from the green emitter to the yellow emitter is the more efficient process at 77 K while back energy transfer from the yellow emitter to the green emitter is the more efficient of the two processes at 298 K. Thus, green emission appears quenched at 77 K while yellow emission is quenched at room temperature (Fig. 5 (insert)). The excitation spectra for the green and yellow emissions are essentially similar (Fig. 5 (insert)), which is consistent with these emissions originating from related excitation processes or thermally equilibrated states.

In conclusion, there is no evidence from comparisons of luminescence characteristics of compounds **1** and **2** (Figs. 3b–3d) with those of **3** and **4** (Fig. 3a) that 3*d*-orbital perturbations arising from second sphere coordination of [NH_4(18-Crown-6)]$^+$ cations around [MX_4]$^{2-}$ anions (Fig. 1 and 2) are large enough to contribute significantly to the kind of dramatic spectral differences seen in Figs. 3–5. The "vortex" supramolecular coordination mode (Fig. 2) of compounds **3** and **4** cannot by itself account for the difference between the spectra of **3** and **4** on one hand and the unusual defect behavior of cubic $F23$ systems (Figs. 3b–3d)

on the other. In view of our recent discovery of emission from Mn^{2+} ions in well-defined seven- and eightfold primary coordination environments (8, 9) the presence of defect sites with Mn^{2+} in primary coordination environments other than ca. T_d $[MX_4]^{2-}$ are the best explanation for the spectral anomalies discussed in items (i)–(iii) above. To throw more light on the dynamics of reversible energy transfer processes of compound **2** as well as the strange electronically active defects featured by cubic $F23$ $[(A(18\text{-Crown-6}))_4MnX_4][BX_4]_2$ generally we studied the temperature evolution of the luminescence decay behavior of compounds **1** and **2**.

Luminescence Decay Dynamics of $[(NH_4(18\text{-}Crown\text{-}6))_4MnBr_4][TlBr_4]_{2(s)}$ (**1**)

Luminescence decay curves ($\lambda_{em} = 512$ nm; $\lambda_{exc} = 479$ nm) of compound **1** are monoexponential and marginally temperature dependent for $60 < T < 120$ K. The emission decay rate at the lowest temperature reached in this study (2.6×10^3 s^{-1} at 60 K) is close to that normally exhibited by unquenched emission from $[MnBr_4]^{2-}$ anions (e.g., 2.6×10^3 s^{-1} for compound **3** or ca. 2.8×10^3 s^{-1} for isolated $[MnBr_4]^{2-}$ anions in inert environments (3, 8, 9)). For comparative purposes, this decay rate (2.6×10^3 s^{-1}) was used as the spontaneous decay rate (k_s) for $[MnBr_4]^{2-}$ in $[(NH_4(18\text{-Crown-6}))_4MnBr_4][TlBr_4]_{2(s)}$. This obviated use of $[ZnBr_4]^{2-}$ to generate dilute environments for $[MnBr_4]^{2-}$ species, such as those expected for $[(NH_4(18\text{-Crown-6}))_4(MnBr_4)_{1-x}(ZnBr_4)_x][TlBr_4]_{2(s)}$, where $x > 0.99$, which carries the risk of introducing new defects known to be associated with $[ZnBr_4]^{2-}$ sites in cubic $F23$ crystals (3). The Arrhenius plot ($\ln k_t = \ln A - E_a/RT$) for $[(NH_4(18\text{-Crown-6}))_4MnBr_4][TlBr_4]_{2(s)}$ (Fig. 6), reveals a triphasic temperature dependent emission decay regime. Here, k_t = quenching rate $= k_{obs} - k_s$; k_{obs} = experimental temperature dependent emission decay rate). We attribute the small thermal barrier at $60 < T < 120$ K, $E_a \approx 1.4 \pm 0.04$ kJ/mol (Fig. 6) to the activation energy for rotational motion of ammonium ions in the $[NH_4(18\text{-Crown-6})]^+$ complex as it is close to the value of ca. 1.3 kJ/mol predicted for this motion in molecular mechanics and dynamical studies of $[NR_4(18\text{-Crown-6})]^+$ (R = H or alkyl group) complexes (10). For $120 < T < 230$ K and $230 < T < 280$ K (Fig. 6) the respective thermal barriers of 7 ± 0.04 and 13 ± 0.2 kJ/mol are similar to those of other cubic $F23$ complexes $[(K(18\text{-Crown-6}))_4MnBr_4[TlBr_4]_{2(s)}$ (ca. 9 kJ/mol) and $[(Rb(18\text{-Crown-6}))_4MnBr_4][TlBr_4]_{2(s)}$ (ca. 8–14 kJ/mol) (3). As for $[(K(18\text{-Crown-6}))_4MnBr_4[TlBr_4]_{2(s)}$ and $[(Rb(18\text{-Crown-6}))_4MnBr_4][TlBr_4]_{2(s)}$, we believe that quenching of $[(NH_4(18\text{-Crown-6}))_4MnBr_4][TlBr_4]_{2(s)}$ emission by crystal defects at $120 < T < 230$ K is triggered by energy migration on the $[MnBr_4]^{2-}$ sublattice. The activation energy of 7–13 kJ/mol (590–1090 cm^{-1}/mol) is in this case required to bridge the energy gap (ca. 700 cm^{-1}) between the emission (Fig. 4) of the Stokes shifted donor $Mn^{2+}(^4T_1(^4G))$ state (ca. 19 500 cm^{-1}) and the origin of the acceptor $Mn^{2+}(^4T_1(^4G) \leftarrow {}^6A_1)$ transition (ca. 20 200 cm^{-1}) on neighboring $[MnBr_4]^{2-}$ ions. There is a rapid increase in emission decay rate at 280 K, which results in emission too weak to measure reliably.

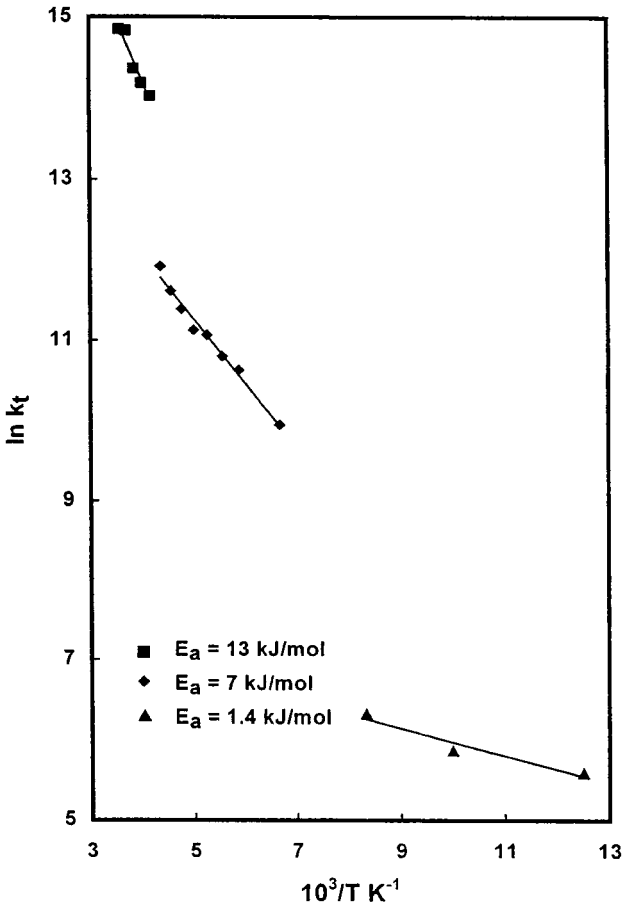

FIG. 6. Arrhenius plot (ln k_t vs $1/T$) (80–280 K) for $[(NH_4(18\text{-Crown-6}))_4MnBr_4][TlBr_4]_{2(s)})$ (**1**). Emission was monitored at 512 nm.

Luminescence Decay Dynamics of $[(NH_4(18\text{-}Crown\text{-}6))_4MnCl_4][TlCl_4]_{2(s)}$ (**2**)

The luminescence decay dynamics of compound $[(NH_4(18\text{-Crown-6}))_4MnCl_4][TlCl_4]_{2(s)}$ (**2**) were particularly interesting because of the temperature dependence of the color of the emitted light (maximum intensity at $\lambda_{em} = 521$ nm for 298 K and 558 nm for 77 K) (Fig. 5 (insert)). The normal $Mn^{2+}(^4T_1(^4G) \rightarrow {}^6A_1)$ green emission was monitored at 510 nm while the orange emission, which we attributed to defect sites, was monitored at 590 nm to minimize mutual interference. The decay behavior of the green emission (510 nm) is single-exponential and

marginally temperature dependent for $T < 180$ K. The decay rate ($k_s = 2.6 \times 10^2$ s^{-1}) at the lowest temperature reached (60 K) was used as the spontaneous rate for comparative purposes. Such k_s values are in fact common for $Mn^{2+}(^4T_1(^4G) \rightarrow {}^6A_1)$ emission from $[MnCl_4]^{2-}$ anions (4a, 11–14). At $T > 180$ K, the decay behavior is more temperature dependent and not single-exponential; decay rates of fast decaying components were in this case estimated from double exponential curve fitting routines and used to study quenching processes. The Arrhenius plot of **2** was found to be triphasic with a thermal barrier of ca. 1.8 ± 0.01 kJ/mol at low temperature ($T < 180$ K), which we again attribute to the solid state rotational motion of the NH_4^+ cation in the $[NH_4(18\text{-Crown-6})]^+$ complex (10). Thermal barrier of 8 ± 0.05 kJ/mol (Fig. 5), which is similar in magnitude to those of other cubic $F23$ members (see discussion of compound **1** above) was found for $180 < T < 250$ K. A thermal barrier of 35 ± 0.7 kJ/mol (Fig. 5) which is of similar magnitude to that of $[(Rb(18\text{-Crown-6}))_4MnBr_4][TBr_4]_{2(s)}$ (ca. 26 kJ/mol) (3) was found for $250 < T < 300$ K.

For the defect emission monitored at 590 nm, luminescence decay behavior is monoexponential ($k_s = 2.5 \times 10^2$ s^{-1}) and temperature independent up to 150 K; for $170 < T < 200$ K luminescence decay behavior is monoexponential but temperature dependent while at $T > 210$ K emission decay behavior is not single-exponential. The temperature dependence of the decay behavior of the defect emission is triphasic, the thermal barriers being ca. 7 ± 0.1 kJ/mol ($150 < T < 200$ K), 8 ± 0.1 kJ/mol ($210 < T < 250$ K) and 29 ± 0.4 kJ/mol ($250 < T < 300$ K) (Fig. 5). Thus, thermal barriers for quenching defect emissions from compounds **2** ($\lambda_{em} = 590$ nm) and $[(K(18\text{-Crown-6}))_4MnBr_4][TlBr_4]_{2(s)}$ ($\lambda_{em} = 610$ nm, ca. 9 kJ/mol) (3) as well as the normal $Mn^{2+}(^4T_1(^4G) \rightarrow {}^6A_1)$ ($[MnX_4]^{2-}$) ($\lambda_{em} = 510$ nm) emissions from **2** and other cubic $F23$ $[(A(18\text{-Crown-6}))_4MnX_4][TlX_4]_{2(s)}$ systems, are of similar magnitude (ca. 7–14 kJ/mol) for $150 < T < 250$ K and 26–35 kJ/mol for $T > 250$ K. Thus, previous detailed arguments (3) used to assign thermally activated quenching processes at $150 < T < 250$ K to rate limiting $Mn^{2+}(^4T_1(^4G))$-to-$Mn^{2+}(^4T_1(^4G))$ energy migration and those of $T > 250$ K to the merry-go-round motion of 18-Crown-6 (15–19) in cubic $F23$ $[(A(18\text{-Crown-6}))_4MnX_4]$ $[TlX_4]_{2(s)}$ crystals are plausible for compounds **1** and **2** too. However, the thermal barrier of (ca. 29 kJ/mol (ca. 2500 cm^{-1}); Fig. 5) for quenching the defect emission (($\lambda_{em} = 590$ nm) at 250 K is close to the energy (ca. 31 kJ/mol (ca. 2600 cm^{-1})) needed to bridge the emitting defect state (maximum emission intensity is at ca. 558 nm (ca. 17 900 cm^{-1})) with the normal $Mn^{2+}(^4T_1(^4G))$ ($[MnCl_4]^{2-}$) absorption origin at ca. 487 nm (ca. 20 500 cm^{-1}), (Fig. 5 (insert)). Quenching of defect emission of **2** at $T > 250$ K may therefore be most limited by the defect-to-normal Mn^{2+} ($^4T_1(^4G)$) ($[MnCl_4]^{2-}$) back energy transfer process rather than solid state 18-Crown-6 motion. This possibility would account more satisfactorily for the prominence of normal green Mn^{2+} ($^4T_1(^4G) \rightarrow {}^6A_1$) emission of $[MnCl_4]^{2-}$ ions from **2** at room temperature, and its defect yellow emission at 77 K (Fig. 5 (insert)).

CONCLUDING REMARKS

The normal behavior of compounds **3** and **4** shows that, on their own, variations in second sphere coordination environments of Mn^{2+} ions in defect supramolecular cations $[(A(18\text{-Crown-6}))_nMnX_4]^{(n-2)+}$ ($n < 4$) cannot account for the diversity in emission and excitation spectral profiles exhibited by cubic $F23$ systems. More significant changes in the primary coordination sphere of Mn^{2+} or completely different species with unpaired electrons are needed to satisfactorily explain the diverse spectral profiles. However, the existance of these defects could be facilitated by the presence of structural defects $[(A(18\text{-Crown-6}))_nMnX_4]^{(n-2)+}$ ($n < 4$) as well as substitutional errors in which $[MnX_4]^{2-}$ are replaced by $[TlX_4]^-$ and vice versa. The resulting charge imbalances may require charge balancing Mn^{2+} cations or electrons occupying strange locations of cubic $F23$ systems to achieve electrical neutrality. These strange Mn^{2+} cations or electron locations could impose spectroscopic characteristics of their own or engage in energy transfer processes with the $[MnX_4]^{2-}$ anions. Caution is required when relating solid state behavior to data from gas phase processes, especially those of exotic environments such as mass spectrometers. But the appearence of $[(NH_4(18\text{-Crown-6}))_2MnBr_4] + NH_4]^+$ ($m/z = 957$, 40%), $[(NH_4(18\text{-Crown-6}))_3MnBr_4]^+$ ($m/z = 1221$, 30%) and $[(NH_4(18\text{-Crown-6}))_2TlBr_4]^+$ ($m/z = 1088$, 100%) species in the Fast Atom Bombardment Mass spectrum of the cubic $F23$ $[(NH_4$ $(18\text{-Crown-6}))_4MnBr_4][TlBr_4]_{2(s)}$ complex (Fig. 7) is consistent with the possible existence of $[(A(18\text{-Crown-6}))_nMnX_4]^{(n-2)+}$ ($n < 4$) defect sites in cubic $F23$ systems. Indeed, the successful isolation and structural characterization of compound **4** and its analogues as well as the elegant Br^- templated assembly of the $[(Na(15\text{-Crown-5}))_4Br]^{3+}$ supramolecular cation (20) reinforces this view. Compounds of the type $[(NH_4(18\text{-Crown-6}))_3MnX_4][TlX_4]$ were sought but not found. Taken together, the results herein reported and our earlier discovery of yellow–green and orange emission from Mn^{2+} in well-defined eight and sevenfold coordination environments (8, 9) point to strange Mn^{2+} environments as the principal origin for electronically active defect sites of the cubic $F23$ crystal systems. The population of defect sites seems to increase with decreasing size of the A^+ ions. For example, compound $[(Rb(18\text{-Crown-6}))_4MnBr_4][TlBr_4]_{2(s)}$ features quenched but normal green $Mn^{2+}(^4T_1(^4G) \rightarrow {}^6A_1)$ emission of $[MnCl_4]^{2-}$ anions while $[(K(18\text{-Crown-6}))_4MnBr_4][TlBr_4]_{2(s)}$ features

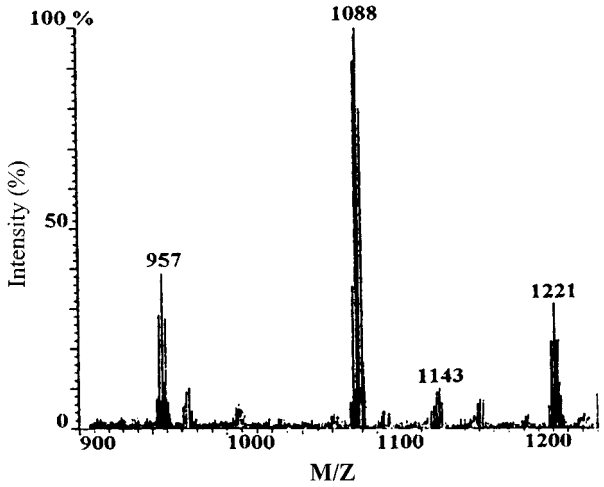

FIG. 7. Fast atom Bombardment Mass spectrum of compound **1**. Assignments: $[(NH_4(18\text{-Crown-6}))_3MnBr_4] + NH_4]^+$ ($m/z = 957$), $[(NH_4(18\text{-Crown-6}))_3MnBr_4]^+$ ($m/z = 1221$), and $[(NH_4(18\text{-Crown-6}))_2TlBr_4]^+$ ($m/z = 1088$).

defect emission only and $[(Na(18\text{-Crown-6}))_4MnBr_4][TlBr_4]_{2(s)}$ is not emissive. Defects are important to the behavior of solid state materials; modification of luminescence (21–26), magnetic properties (27), semiconductor energy band gaps (28), dielectric relaxation processes (29) and crystal structure (30, 31) are some of the more common manifestations of defect activity.

ACKNOWLEDGMENTS

We thank the Chemistry Department UWI for a demonstratorship and a departmental award to N.S.F., the Inter-American Development Bank-UWI Development Program (R&D Project No. 29) for supporting the luminescence work at UWI, the Forensic laboratory (Jamaica) for a loan of the LS5 spectrometer and John Barton of Imperial College for help with the FAB MS analyses.

REFERENCES

1. I. A. Kahwa, D. Miller, M. Mitchell, F. R. Fronczek, R. G. Goodrich, D. J. Williams, C. A. O'Mahoney, A. M. Z. Slawin, S. V. Ley, and C. J. Groombridge, *Inorg. Chem.* **31,** 3963 (1992).
2. N. S. Fender, S. A. Finegan, D. Miller, M. Mitchell, I. A. Kahwa, and F. R. Fronczek, *Inorg. Chem.* **33,** 4002 (1994).
3. N. S. Fender, F. R. Fronczek, V. John, I. A. Kahwa, and G. L. McPherson, *Inorg. Chem.* **36,** 5539 (1997).
4. (a) R. A. Fairman, W. A. Gallimore, K. V. N. Spence, and I. A. Kahwa, *Inorg. Chem.* **33,** 823 (1994); (b) A. D. Kirk, H.-L. Schlaffer, *J. Chem. Phys.* **52,** 2411 (1970).
5. I. A. Kahwa, D. Miller, M. Mitchel, and F. R. Fronczek, *Acta Crystallogr. Sect. C: Cryst. Struct. Commun.* **49,** 320 (1993).
6. N. S. Fender, *Ph. D. thesis*, University of the West Indies, Mona Campus, Jamaica, 1997.
7. M. T. Vala, C. J. Ballhausen, R. Dingle, and S. L. Holt, *Mol. Phys.* **23,** 217 (1972).
8. H. O. N. Reid, I. A. Kahwa, A. J. P. White, and D. J. Williams, *Inorg. Chem.* **37,** 3868 (1998).
9. H. O. N. Reid, I. A. Kahwa, A. J. P. White, and D. J. Williams, *Chem. Commun.* 1565 (1999).
10. D. Gehin, P. A. Kollman, and G. Wippf, *J. Am. Chem. Soc.* **111,** 3011 (1989).
11. M. Writon and D. Ginley, *Chem. Phys.* **4,** 295 (1974).
12. N. Presser, M. A. Ratner, and B. R. Sundheim, *Chem. Phys.* **31,** 281 (1978).
13. I. Buric, K. Nicolac, and A. Aleksic, *Acta Phys. Pol. A* **69,** 561 (1986).
14. M. C. Marco de Lucas and F. Rodriquez, *J. Phys. Condens. Matter* **1,** 4251 (1989).
15. C. I. Ratcliffe, J. A. Ripmeester, G. W. Buchanan, and J. K. Denike, *J. Am. Chem. Soc.* **114,** 3294 (1992).
16. G. W. Buchanan, C. Morat, C. I. Ratcliffe, and J. A. Ripmeester, *J. Chem. Soc. Chem. Commun.* 1306 (1989).
17. M. J. Wagner, L. E. H. McMills, A. S. Ellaboudy, J. S. Elgin, J. L. Dye, P. P. Edwards, and N. C. Pyper, *J. Phys. Chem.* **96,** 9656 (1992).
18. C. I. Ratcliffe, G. W. Buchanan, and J. K. Denike, *J. Am. Chem. Soc.* **117,** 2900 (1995).
19. J. L. Dye, *Inorg. Chem.* **36,** 3816 (1997).
20. N. S. Fender, I. A. Kahwa, A. J. P. White, and D. J. Williams, *J. Chem. Soc. Dalton Trans.* 1729 (1998).
21. A. A. Bol and A. Meijerink, *Phys. Chem. Chem. Phys.* **3,** 2105 (2001).
22. J. F. Suvyer, S. F. Wuister, J. J. Kelly, and A. Meijerink, *Phys. Chem. Chem. Phys.* **2,** 5445 (2000).
23. H. B. Kim, T. G. Kim, J. H. Son, C. N. Whang, K. H. Chae, W. S. Le, S. Im, and J. H. Song, *J. Appl. Phys.* **88,** 1851 (2000).
24. P. S. Pizani, E. R. Leite, F. M. Pontes, E. C. Paris, J.-H. Rangel, E. J. H. Lee, E. Longo, P. Delega, and J. A. Varela, *Appl. Phys. Lett.* **77,** 824 (2000).
25. M. de Castro Jimenez, R. Serna, J. A. Chaos, C. N. Afonso, and E. R. Hodgeson, *Nucl. Instrum. Methods Phys. Res. Sect. B* **166–167,** 793 (2000).
26. W. Li, D. Mao, F. Zhang, X. Wang, X. Liu, S. Zou, Y. Zhu, Q. Li, and J. Xu, *Nucl. Instrum. Methods Phys. Res. Sect. B* **169,** 59 (2000).
27. S. Schweizer, U. Rogulis, K. S. Song, and J.-M. Spaeth, *J. Phys. Condens. Matter* **12,** 6237 (2001).
28. I. A. Buyanova, W. M. Chen, B. Monemar, H. P. Xin, and C. W. Tu, *Mater. Sci. Eng. B* **75,** 166 (2000).
29. E. Elissalde and J. Ravez, *J. Mater. Chem.* **11,** 1957 (2001).
30. E. T. Maguire, A. M. Coats, J. M. S. Skakle, and A. R. West, *J. Mater. Chem.* **9,** 1337 (1999).
31. R. E. Schaak, E. N. Guidry, and T. E. Mallouk, *Chem. Commun.* 853 (2001).